Available online at www.sciencedirect.com

SciVerse ScienceDirect

Physics Procedia 37 (2012) 606 – 612

Physics Procedia

TIPP 2011 - Technology and Instrumentation for Particle Physics 2011

The Ring Imaging CHerenkov detectors of the LHCb experiment

Davide Luigi Perego[1]

Università degli Studi di Milano–Bicocca and INFN, Piazza della Scienza 3, Milano, I–20126, Italy

Abstract

Particle identification is a fundamental requirement of the LHCb experiment to fulfill its physics programme. Positive hadron identification is performed by two Ring Imaging CHerenkov (RICH) detectors. This system covers the full angular acceptance of the experiment and is equipped with three Cherenkov radiators to identify particles in a wide momentum range from 1 GeV/c up to 100 GeV/c. The Hybrid Photon Detectors (HPDs) located outside the detector acceptance provide the photon detection with 500,000 channels. Specific read–out electronics has been developed to readout and process data from the HPDs including data transmission and power distribution. The operation and performance of the RICH system are ensured by the constant control and monitoring of low and high voltage systems, of the gas quality and environmental parameters, of the mirror alignment, and finally of the detector safety. The description of the LHCb RICH is given. The experience in operating the detector at the Large Hadron Collider is presented and discussed.

Keywords: RICH detectors, Hybrid photon detectors, LHCb experiment
PACS: 29.40.Ka, 42.79.Pw, 85.60.Gz

1. Introduction

The LHCb experiment physics programme is focused on the search for New Physics beyond the Standard Model through precise studies of CP violation and rare decays in the heavy flavour sector [1]. The geometry of the detector [2] is optimized on the particular forward–backward distribution of the produced $b\bar{b}$ pairs and it consists of a single arm spectrometer with an angular acceptance coverage up to 300 (250) mrad in the horizontal (vertical) plane. It is designed to exploit the large production cross-section of b quarks at the proton–proton Large Hadron Collider (LHC) running at CERN.

[1]On behalf of the LHCb RICH Collaboration. Email: Davide.Perego@mib.infn.it

 doi:10.1016/j.phpro.2012.02.414

Table 1. Properties of the LHCb RICH radiators and expected performance (angular resolution and photoelectron yield) from full simulation data.

	Aerogel	C_4F_{10}	CF_4
Length (cm)	5	85	167
Refractive index	1.03	1.0014	1.0005
Momentum (GeV/c)	1–10	up to 40	up to 100
$\sigma^{tot}(\theta_C)$ (mrad)	2.6	1.5	0.7
$\mathcal{N}_{pe}$/track	6.7	30.3	21.9

2. The RICH system

Particle identification is essential to distinguish charged particles for trigger and flavour tagging purposes and to enhance the high purity selection of the final states relevant for CP violation studies. Two Ring Imaging CHerenkov detectors (RICH 1 and RICH 2) provide positive $\pi - K$ separation in the wide momentum range 1–100 GeV/c, using three radiators (solid silica aerogel, C_4F_{10} and CF_4 gas) suitably chosen for the different momentum ranges of interest [2]. Their main properties are summarized in Table 1.

The layouts of the two detectors are similar (RICH 2 is rotated by 90° in the vertical plane with respect to RICH 1). The Cherenkov photons produced by charged tracks going through the radiators are focused by a set of tilted spherical mirrors onto the photon detection planes located outside the geometrical acceptance. A set of flat mirrors have been introduced to shorten the length of the detectors along the beam axis direction. The photon detectors are placed inside magnetic shielding boxes to limit the distortion induced by the fringes of the magnetic field from the dipole of the experiment.

3. The photon detection system

The Cherenkov photons are detected by a set of 484 pixel Hybrid Photon Detectors (HPDs) [3]. A pixel HPD consists of a pixelated silicon sensor, bump–bonded to a read–out chip and encapsulated into a vacuum tube. The photons are converted into photoelectrons by a thin layer of multi–alkali S20 photocathode deposited on the inner surface of a quartz spherical entrance window. The photocathode sensitivity ranges from 200 nm to 600 nm and has been optimized to minimize the chromaticity effects of the Cherenkov

Fig. 1. Pixel Hybrid Photon Detectors (HPDs) integrated in one box of the RICH 1 detector. The hexagonally packing is clearly visible.

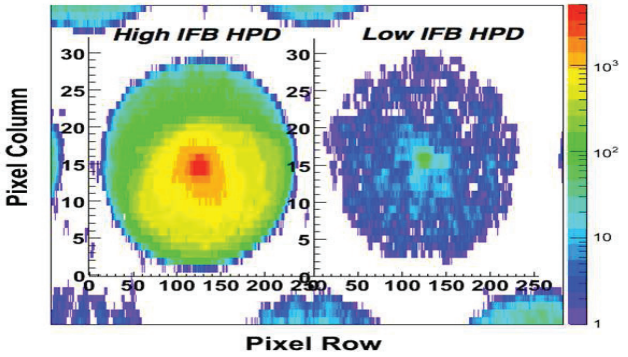

Fig. 2. Comparison of two HPDs showing high (left) and low (right) ion feedback rates.

media. The photoelectrons are accelerated by –18 kV applied to the photocathode and cross–focused onto the silicon sensor with a demagnification factor of five. The average quantum efficiency improved during the production phase, increasing from ∼23% up to ∼35% at 270 nm. The effective pixel size is 2.5 × 2.5 mm^2 at the photocathode level, for a total coverage surface of ∼3.5 m^2 and an acvtive fraction of 65%. The contribution to the total resolution from the pixel granularity is small. The HPDs are integrated in the detectors in a hexagonally packed fashion, clearly visible in Fig. 1.

These photon detectors are currently showing excellent performance. In particular, they present a very low dark count rate, at an average level of 0.04 photoelectrons per event per HPD (limited thermo–ionic emission of the photocathode and low–noise front–end electronics), so that the noise (*i.e.* the amount and the spatial distribution of background hits) in each event is small.

An important feature of vacuum tubes is the ion feedback (IFB) effect [3]. This phenomenon consists in the ionization of residual gas atoms by the accelerated photoelectrons: the produced ions are accelerated back to the photocathode and several photoelectrons are extracted and accelerated to the anode. This signal is detected with ∼250 ns delay. It has been observed that the quality of the vacuum rapidly degrades over time for a subset of tubes, inducing a corresponding fast increase of the IFB rate[2]. Therefore *in–situ* measurements with a continuous wavelength laser (λ = 635 nm) are periodically carried out. A dedicated off–line analysis is performed to check the temporal evolution of the IFB rate. About 80% of the HPDs shows an IFB lower than 5%, with a yearly increase of ∼0.5%. In case of highly degraded vacuum quality (*i.e.* IFB rate greater than 5%), the adopted strategy is to replace the concerned HPDs. In Fig. 2 the IFB signature (from dark count data) of two HPDs is given.

4. Performance with data

The quality of data taken by the RICH system is excellent. Fig. 3 and Fig. 4 show the typical scenario during data taking. The signal is clear, and the background level is really limited. The performance achieved is close to the design one. The most important key features are listed in the following:

1. DAQ time alignment;
2. spherical and flat mirrors alignment;
3. magnetic distortion corrections;
4. calibration of the gaseous refractive indices (temperature, pressure and gas composition);
5. calibration of the refractive indices of the aerogel tiles;

[2]IFB measurements are defined by counting clusters of hits. A single photoelectron from a signal Cherenkov photon can conceivably register hits in up to four neighbouring pixels if it lands in a corner. Therefore incidents where ≥ 5 adjacent pixels are hit in the same event are considered as IFB. The rate of IFB is defined as the ratio of such a large clusters to all clusters accumulated over all events.

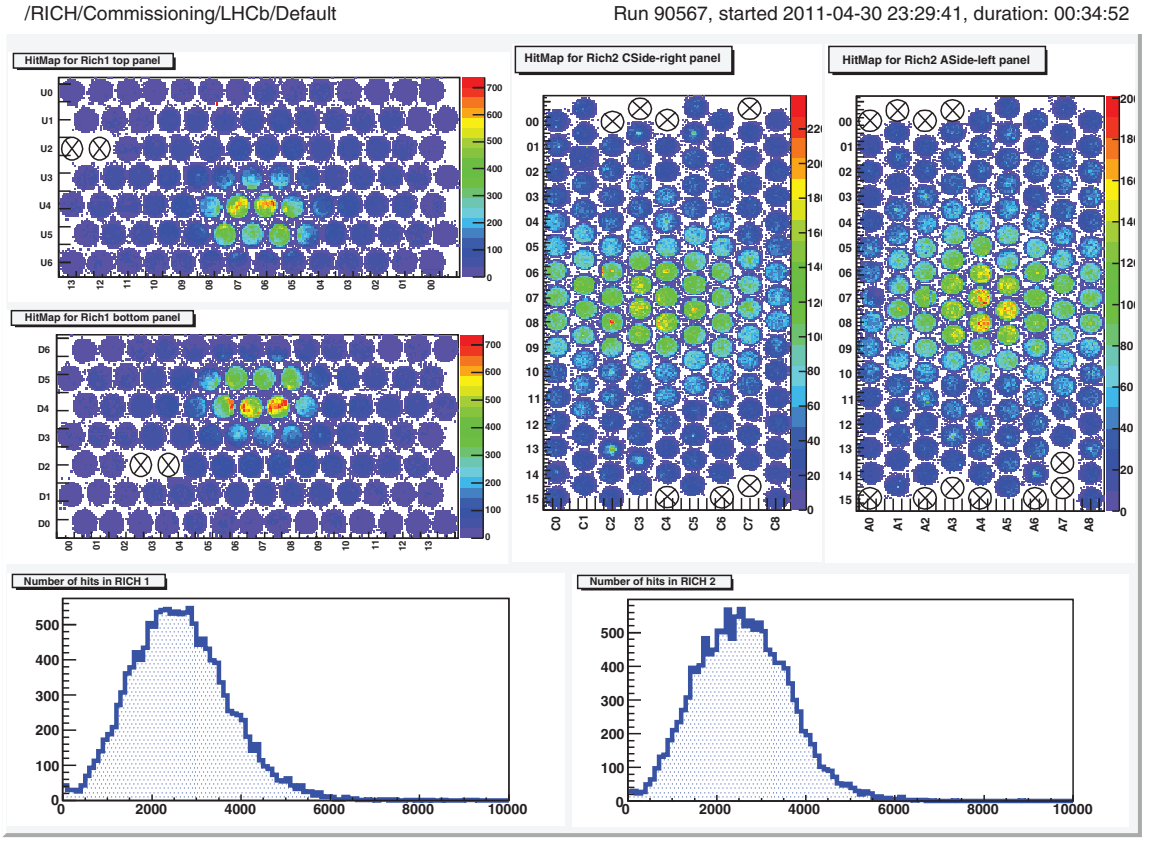

Fig. 3. On–line event display. RICH 1 is on the left side, RICH 2 on the right. Cherenkov hits are accumulated over many events; each circle corresponds to an HPD. The color scale shows the occupancy is not uniform over the photon detection planes. This is the consequence of the layout of the optical system and of the refractive indices of the radiators. At the bottom, typical hit multiplicity of RICH 1 and RICH 2 respectively.

6. HPD imaging calibration.

The full description of the alignment and the calibration and their consequences on physics analysis can be found elsewhere [4]. Here only a short overview of selected issues is given.

All the HPDs and their read–out have been carefully time aligned to maximize the detection efficiency well within a bunch crossing interval. The temporal distributions of all the HPDs are very sharp and have an excellent time resolution of about 0.5 ns.

The gaseous radiators conditions and compositions directly affect the resolution of the Cherenkov angle. The gases temperatures and pressures follow the atmospheric variations and the overall precision of the gas system is ~0.1 hPa. The actual compositions of the two gas radiators are periodically checked with dedicated measurements from chromatography. The typical purity of RICH 1 C_4F_{10} is above 99%. In RICH 2 the percentage of CF_4 is set at the level of 93%, where the remaining part is CO_2, which is added to suppress the CF_4 scintillation light induced by the traversing particles. An off–line fine calibration with data is performed on a run–by–run basis to match the correct refractive index.

Considering all the building blocks listed at the beginning of this Section, the 2010 data performance of the gas radiators are $\sigma_\theta = 1.62$ mrad (RICH 1) and $\sigma_\theta = 0.68$ mrad (RICH 2). These numbers are in good agreement with expectations listed in Tab. 1. The resolutions present also an excellent stability over the full year of data taking.

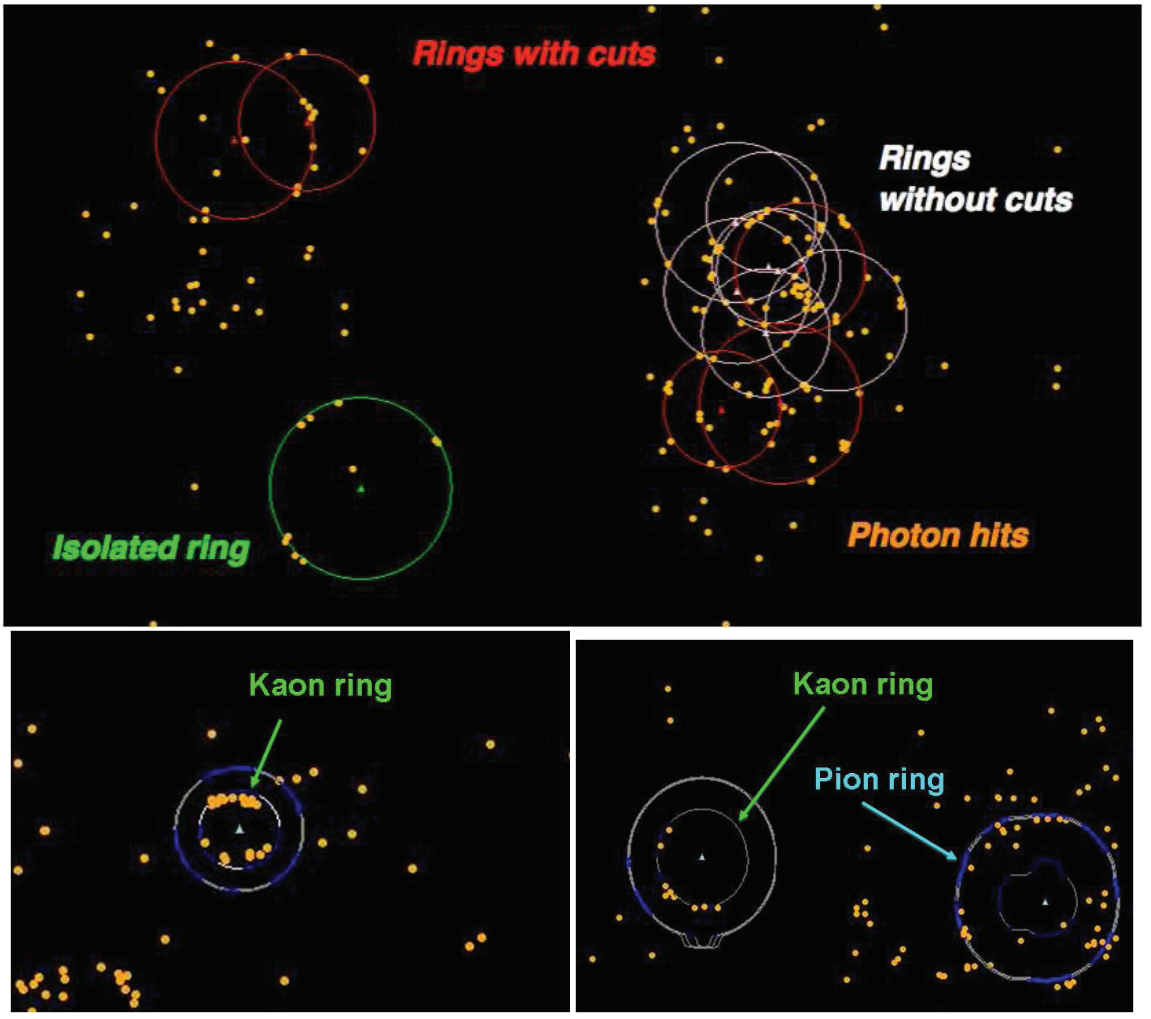

Fig. 4. On–line visualization of Cherenkov hits and reconstructed rings. The signal is clear and nice. In these images, from both RICH 1 (top) and RICH 2 (bottom), different algorithm and mass hypothesis have been applied, for a quick cross–check of the performance of the system. The whole RICH 1 image has been rotated by 90°.

The expected final Cherenkov angle resolution of the silica aerogel radiator has not yet been achieved. A shift of the mean value of θ_C and a worse overall resolution with respect to the expected ones have been observed.

The aerogel radiator is not hermetically sealed inside RICH 1, but it is in contact with gaseous C_4F_{10}. This replaces the dry air trapped inside the porous structure. The absorption is quite fast in time and it is proportional to the surface of the internal pores and cause a change in the optical properties. Both the refractive index and the clarity factor[3] are affected. The worsening induced by the absorbed C_4F_{10} consists in:

1. enhancement of the forward scattering (therefore degradation of the resolution);
2. reduction of the photoelectron yield.

[3]The clarity factor is the parameter used to describe the Rayleigh scattering of light inside an aerogel block. It is inversely proportional to the scattering length [5].

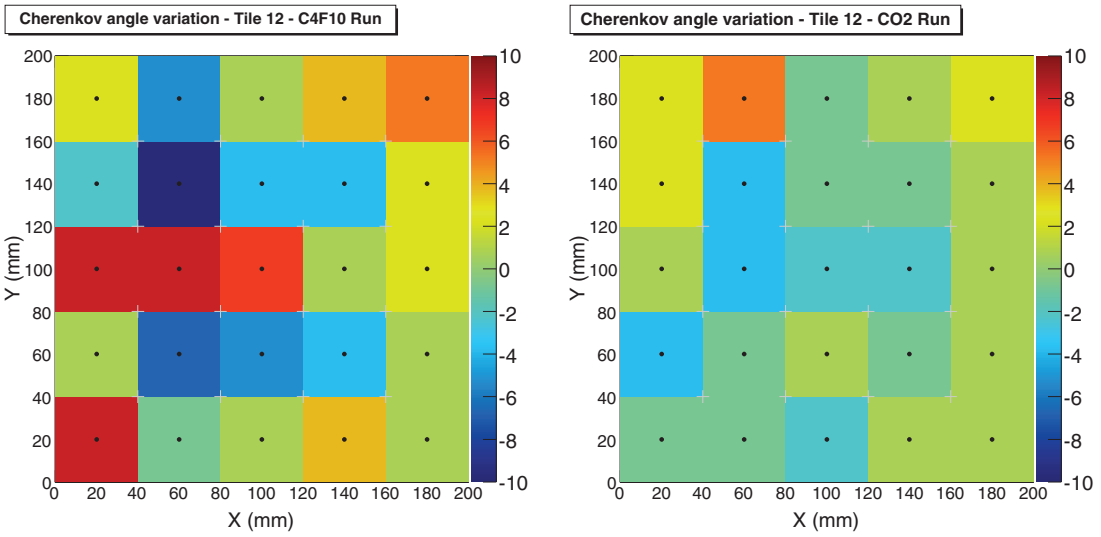

Fig. 5. $\Delta\theta_C$ offset of an aerogel tile subdivided into 25 smaller segments. The offset is determined with respect to the expected value of θ_C of the particular block of aerogel considered. The variation of $\Delta\theta_C$ follows the inhomogeneity of the density inside the block. On the left, variation from data taken when C_4F_{10} was filling the RICH 1 gas enclosure; on the right, variation during the CO_2 run test. The same aerogel tile has been considered for this comparison. The effect of the absorbed C_4F_{10} is clearly visible.

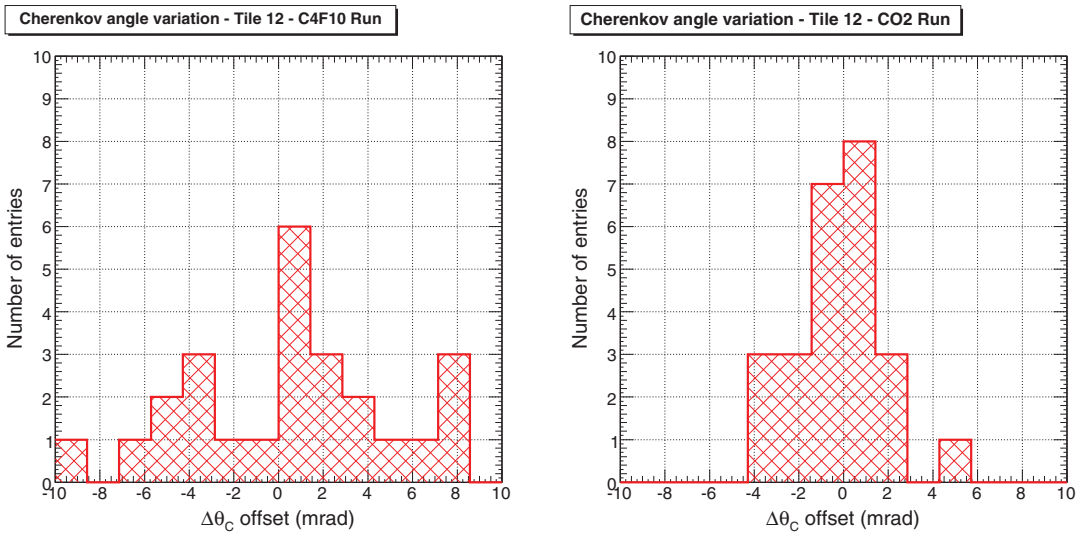

Fig. 6. Histogram distributions of the $\Delta\theta_C$ offsets of the aerogel block considered in the paragraph. On the left, distribution from data taken when C_4F_{10} was filling the RICH 1 gas enclosure; on the right, histogram obtained during the CO_2 run test. The same aerogel tile has been considered for this comparison. The effect of the absorbed C_4F_{10} is clearly visible.

From laboratory tests [6] the additional scattering contribution is $\sim$ 3.4 mrad while the photoelectron loss is up to -25%. This numbers can explain the present performance of the aerogel below the Monte–Carlo expectations.

A test run with CO_2 replacing C_4F_{10} was carried out at the beginning of 2011 data taking. The main result is that the optical conditions and performance of the aerogel are improved, although the complete analysis is still ongoing. A gas–tight housing box which will totally separate the two Cherenkov media in

RICH 1 is currently under construction and it will be installed during the next LHC stop at the end of the year. For the time being, the performance of aerogel are maximized at the event reconstruction level, with a run–by–run calibration of the refractive index of each single tile.

An improvement of the resolution has been obtained considering the local variation of the refractive index inside a given tile. The density of the aerogel is not uniform [7], and this non–uniformity is enhanced by the C_4F_{10} absorption, producing a further worsening of the resolution. Fig. 5 shows the $\Delta\theta_C$ offset measured with 2010 data subdividing a tile in several smaller sub–tiles. For the run considered, the spread is 4.7 mrad. For the same tile, during the CO_2 run test, this spread is reduced down to 2.1 mrad. These spreads are clearly visible in the histograms shown in Fig. 6. The strategy adopted now is to include in the reconstruction software this feature, and to calibrate, on a run–by–run basis, each sub–tiles. Results will be available soon.

5. Conclusions

The RICH system of the LHCb experiment is providing powerful particle identification, given to the very low noise of the electronics and of the photon detectors and to the excellent calibration and alignment. The system is running smoothly and the performance achieved with the first data taken are close to the expectations.

References

[1] The LHCb Coll., Roadmap for selected key measurements of LHCb, arXiv:0912.4179v2 [hep–ex]
[2] The LHCb Coll., The LHCb Detector at the LHC, 2008 JINST 3 S08005
[3] R. Young, Nucl. Instr. and Meth. A 639 (2011) 94
[4] A. Papanestis, Performance of the RICH detectors of LHCb, these proceedings
[5] A. J. Hunt, et al., Mater. Res. Soc. Symp. Proc. 32 (1984) 275
[6] D. L. Perego, Nucl. Instr. and Meth. A 639 (2011) 234
[7] T. Bellunato, et al., Nucl. Instr. and Meth. A 556 (2006) 140